American Society of Mechanical Engineers, New York (1962).
18. ———, *A.I.Ch.E. Journal*, **6**, 631 (1960).
19. *Ibid.*, **7**, 423 (1961).
20. Allred, V. D., S. R. Buxton, and J. P. McBride, *J. Phys. Chem.*, **61**, 117 (1957).
21. Boyd, C. M., et al., *Oak Ridge National Laboratory Report ORNL-2345* (August 5, 1957).
22. Herdan, G., "Small Particle Statistics," Elsevier Publishing Co., Amsterdam, Netherlands (1953).
23. Smellie, R. H., Jr., and V. K. LaMer, *J. Colloid Sci.*, **11**, 720 (1956).
24. Hoskin, N. E., and Samuel Levine, *Phil. Trans.*, **A248**, 449 (1955).
25. Derjaguin, B. V., *Kolloid-Z.*, **69**, 155 (1934).
26. Reerink, H., and J. Th. G. Overbeek, *Disc. Faraday Soc.*, No. 18, 74 (1954).
27. Davies, J. T., and E. K. Rideal, "Interfacial Phenomena," Academic Press, New York (1961).
28. Koelmans, H., and J. Th. G. Overbeek, *Disc. Faraday Soc.*, No. 18, 52-63 (1954).
29. Hamaker, H. C., *Physica*, **10**, 58 (1937).
30. Verwey, E. J. W., and J. Th. G. Overbeek, "Theory of the Stability of Lyophobic Colloids," Elsevier Publishing Co., New York (1948).
31. Overbeek, J. Th. G., and M. J. Sparnaay, *Disc. Faraday Soc.*, No. 18, 12-24 (1954).
32. Black, W., J. G. V. de Jongh, J. Th. G. Overbeek, and M. J. Sparnaay, *Trans. Faraday Soc.*, **56**, 1597 (1960).
33. Bradley, R. S., *Disc. Faraday Soc.*, No. 18, 182 (1954).
34. Goodeve, C. F., *Trans. Faraday Soc.*, **35**, 342 (1939).
35. Gillespie, Thomas, *J. Colloid Sci.*, **15**, 219 (1960).
36. Manley, R. St. J., and S. G. Mason, *ibid.*, **7**, 354 (1952).
37. Smoluchowski, M. von, *Physik. Z.*, **17**, 557, 583 (1916).
38. Bartok, W., and S. G. Mason, *J. Colloid Sci.*, **12**, 243 (1957).
39. Burgers, J. M., "Second Report on Viscosity and Plasticity," pp. 113-184, Academy of Sciences, Amsterdam, Netherlands (1938).

Manuscript received September 14, 1962; revision received November 7, 1962; paper accepted November 9, 1962.

Semifluidization in Solid-Gas Systems

CHIN-YUNG WEN and SHIH-CHUNG WANG
West Virginia University, Morgantown, West Virginia

LIANG-TSENG FAN
Kansas State University, Manhattan, Kansas

A new type of solid-fluid contacting device consisting of the features of both fixed and fluidized beds has been proposed (2, 3). The expansion of a fluidized bed is partially restricted by placing a porous plate or screen on top of the bed. Thus a packed section is formed beneath the top porous plate while the particles underneath remain fluidized. Such an operation is called *semifluidization* (2, 3).

A semifluidized bed has the advantages of both a fluidized and fixed bed. By adjusting the position of the top sieve plate a semifluidized bed can be made to suit any particular chemical reaction.

The mechanics of semifluidization of single size particles has been reported, and the data for solid-liquid systems were correlated (2). It is the purpose of the present investigation to extend the study to solid-gas systems and to present a unified correlation for both solid-liquid and solid-gas systems.

By means of a material balance between the fully fluidized and partially expanded states of the suspension, Fan, Yang, and Wen (3) derived the following equation, assuming that the particles in a column behave independently and uniformly and that the voidage of the packed section is constant:

$$h_{pa} = (h_f - h)(1 - \epsilon_f)/(\epsilon_f - \epsilon_{pa}) \quad (1)$$

The work done by Liang-tseng Fan at Kansas State University was supported by National Science Foundation Grant No. G-14300.

Fan and Wen (2) showed that Equation (1) is valid for any particle shape provided that the particles can be represented by the same characteristic dimensions. Their experimental data substantiated the validity of Equation (1) for large-and-irregular-size particles of benzoic acid in liquid systems.

The total pressure drop across a semifluidized bed can be considered to be equal to the algebraic sum of the pressure drops across the packed section and the fluidized section.

Accordingly

$$\Delta P_t = \Delta P_f + \Delta P_{pa} = (\Delta P/L)_f (h - h_{pa}) + (\Delta P/L)_{pa} h_{pa} \quad (2)$$

When one employs the Ergun equation (1) for the pressure drop in the packed section, the following equation is obtained for the total pressure drop across a semifluidized bed:

$$\Delta P_t = (1 - \epsilon_f)(\rho_s - \rho_f)\left[h_f - \frac{(1 - \epsilon_{pa})(h_f - h)}{(\epsilon_f - \epsilon_{pa})}\right] + \left[150\frac{(1 - \epsilon_{pa})^2}{\epsilon_{pa}^3}\frac{\mu u}{D_p^2} + 1.75\frac{1 - \epsilon_{pa}}{\epsilon_{pa}^3}\frac{Gu}{D_p}\right] \cdot \left[(h_f - h)\frac{1 - \epsilon_f}{\epsilon_f - \epsilon_{pa}}\right] \cdot \frac{1}{g_c} \quad (3)$$

In order to evaluate the total pressure drop in a semifluidized bed by Equation (3), accurate knowledge of fluidized bed porosity as well as fixed bed porosity at the given condition is necessary.

EXPERIMENTAL

The experiments were carried out with the equipment shown schematically in

TABLE 1. PROPERTIES OF SOLID PARTICLES USED IN THE EXPERIMENTS

Particles	D_p, in. (geometrical mean)	Shape	Sphericity ϕ	Absolute density, ρ_s lb./cu. ft.	Porosity of least dense static bed ϵ_o
80- to 100-mesh glass beads	0.0061	Sphere	1.00	156.0	0.4386
High-density polyethylene	0.0663	Sphere segment (diameter 0.1042 in. thickness 0.04218 in.)	0.770	57.87	0.4893
High-density polyethylene	0.1145	Cylinder (diameter 0.1077 in., length 0.1222 in.)	0.867	57.87	0.4448

TABLE 2. CALCULATED AND OBSERVED ONSET VELOCITIES OF FLUIDIZATION

Particles	P_1, lb./sq. in. abs.	Calculated G_{mf}, lb./hr.-sq. ft.	Observed G_{mf}, lb./hr.-sq. ft.	Diameter of particle used in Equation (4)
80- to 100-mesh glass beads	15.1	22.7	18.0	$D_p = 0.0061$ in.
	19.0	28.3	25.0	
	24.2	35.3	30.0	
	27.0	38.9	35.0	
Polyethylene sphere segments	14.6	550	500	Diameter of sphere segment (0.1042 in.)
	17.1	620	600	
	18.3	634	600	
Polyethylene cylinders	14.5	654	600	$D_e = 0.1282$ in.
		602		$D_p = 0.1145$ in.
	16.6	729	730	$D_e = 0.1282$ in.
		704		$D_p = 0.1145$ in.

Figure 1. A two-way stopcock was provided on the low-pressure side of the manometer so that both the pressure drop across the semifluidized bed and the pressure at the bottom of the bed could be obtained. Air was used as a fluidizing medium. The characteristics of the solid particles used are listed in Table 1. Canvas cloth was used as compressing and supporting screens for glass beads, while brass-wire screens were used for polyethylene particles. The pressure drops across the brass-wire screens were negligible compared with the pressure drop across the bed.

After a weighed quantity of solid particles was charged into the glass column, the bed was fluidized with air and allowed to resettle by slowly reducing the air rate to zero. In this way the reproducible readings of the initial static bed height were obtained. The air velocity was then gradually increased up to a point at which the desired compression of the fluidized bed was produced. It is important to increase the air velocity very gradually; otherwise the packed section already formed will become compressed, and the assumption that the porosity of the packed section is constant and equal to that of the least dense static bed will become questionable. Upon reaching the steady state operation the overall pressure drop, the pressure at the bottom of the bed, the height of the packed section, and the operating conditions were recorded.

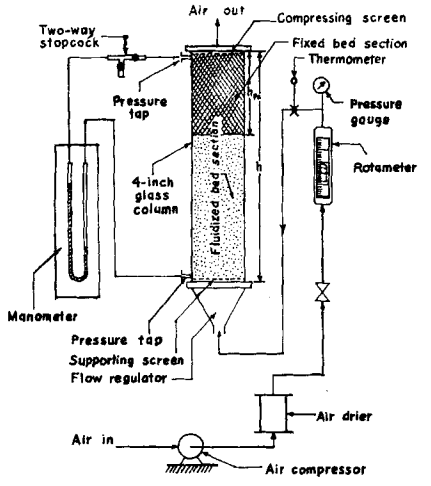

Fig. 1. Schematic diagram of experimental equipment.

The fully fluidized bed experiments were conducted under the same operating conditions. Since air is compressible and the pressure in the semifluidized bed increases as the air velocity is increased, experiments with the fully fluidized bed were carried out under different bed pressures. A regulator valve was mounted on the top of the column so that the pressure at the bottom of the fully fluidized bed could be kept constant by adjusting the amount of outlet air through the valve.

In both semifluidization and fluidization experiments the outside wall of the glass column was heavily coiled with brass wire, one end of which was grounded in order to reduce as much as possible the static electricity induced.

DISCUSSION AND CORRELATION

Examples of the porosities of fully fluidized beds at various air velocities are shown in Figures 2 and 3. Such plots are used for interpolation and extrapolation, required in the analysis of semifluidization data. For the same air mass velocity the higher the bed pressure (P_1 = pressure at the bottom of the bed) the smaller the porosity of the fluidized beds. However, if the correlation is based on linear velocity of the gas as shown in Figure 2, the pressure effect on porosity disappears. Figure 3 shows the effect of bed weight (or initial static bed height) on the bed porosity for polyethylene cylinders.

It is evident that G_{mf} (corresponding to the porosity of least dense static bed ϵ_o) is essentially independent of the bed weight, which agrees with an equation for the onset of fluidization (6, 7). The effect of the bed weight on the porosity becomes progressively smaller after the onset of slugging.

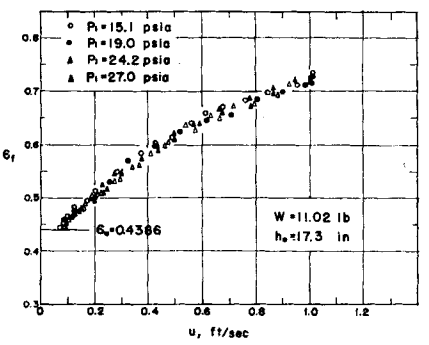

Fig. 2. Porosity of fully fluidized bed of 80- to 100-mesh glass beads with respect to superficial linear velocity of fluid.

The calculated velocities for the onset fluidization with Equation (4) and the observed values by extrapolating the porosity vs. air rate curves to $\epsilon_f = \epsilon_o$ are listed in Table 2:

$$G_{mf} = 688\, D_p^{1.82}\, [\rho_f\, (\rho_s - \rho_f)]^{0.94}/\mu^{0.88} \qquad (4)$$

Equation (4) must be corrected if the resulting $D_p\ G_{mf}/\mu$ is larger than 10 (6, 7). The units of D_p and μ in Equation (4) are inches and centipoise respectively.

Height of Packed Section

Figure 4 shows the observed heights of the packed section as they are plotted against those calculated in accordance with Equation (1). ϵ_{pa} in Equation (1) was assumed to be equal to ϵ_o. Quantities h_f and ϵ_f were obtained from the fluidization data at the corresponding air velocity and pressure by interpolation or extrapolation. The data shown in Figure 4 are more scattered than those for solid-liquid systems (2, 3). At higher air velocities (for example h_{pa} was observed to be larger than 9 in.), the calculated heights of the packed section are consistently smaller than the observed values. This is probably due to the fact that the extrapolated porosity values of the fluidized bed were smaller than the actual values. The height of the fluidized bed fluctuated considerably at a high air rate. It was more logical therefore to use the maximum fluidized bed height instead of the average bed height in the study of semifluidization, since a packed section forms as soon as the surface of the fluidized bed reaches the sieve plate located at the top of the

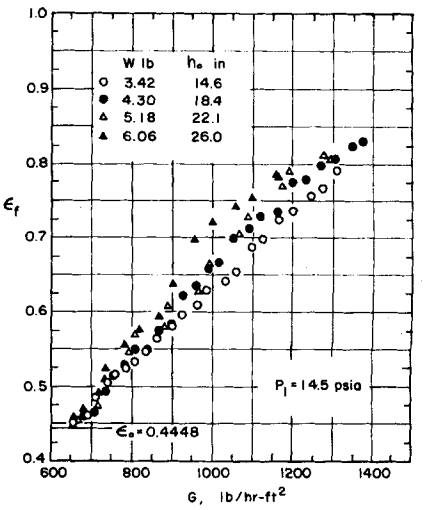

Fig. 3. Effect of bed weight on the porosity of fully fluidized bed (polyethylene cylinders).

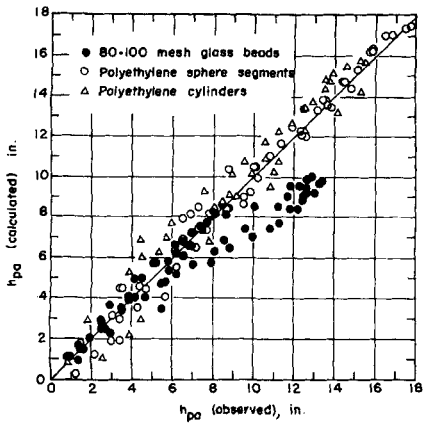

Fig. 4. Comparison of observed heights of packed section with theoretical values.

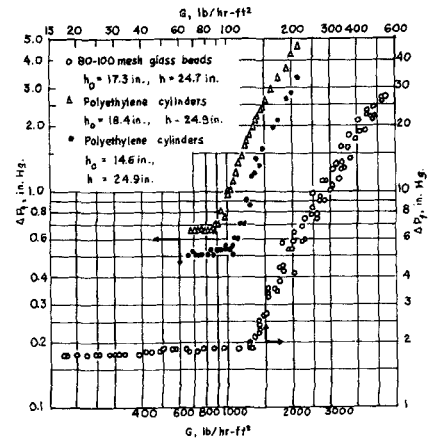

Fig. 5. Overall pressure drops across semifluidized beds (80- to 100-mesh glass beads and polyethylene cylinders).

column. When the bed height is fluctuating, this corresponds to the maximum height of the bed at the given gas rate. The results of the correlation showed that the use of the maximum height was to be preferred. Also the packed section of the glass beads was compressed more severely than that of the dumped static bed of polyethylene particles owing to larger pressure gradient. Therefore the assumption that ϵ_{pa} is equal to ϵ_o is not strictly true.

Maximum Semifluidization Velocity

The maximum flow rate of air at which semifluidization is possible or maximum fluidization velocity corresponds to the terminal velocity of the particles. At an air velocity above this point all the particles will be in the packed section. Therefore the maximum semifluidization velocity may be evaluated by extrapolating the h_{pa}/h_o vs. G curve to $h_{pa}/h_o = 1.0$.

Table 3. Maximum Semifluidization Velocity in 4-in. Column

Particles	Calculated G_t, lb./hr.-sq. ft.	Extrapolated G_t', lb./hr.-sq. ft.	Observed G_t'', lb./hr.-sq. ft.
80- to 100-mesh glass beads	1,200	1,450	2,064
Polyethylene sphere segments	3,380	3,850	3,776
Polyethylene cylinders	5,250	5,600	5,488

Table 4. Pipe Reynolds Numbers and Single Particle Reynolds Numbers

Particle	Pipe D_tG_t''/μ	Particle D_pG_t''/μ
80- to 100-mesh glass beads	15,794	24
Polyethylene sphere segment	28,895	479
Polyethylene cylinder	41,996	1,202

The terminal velocity for a single particle falling in an infinite fluid medium can be calculated by Stokes' law, the intermediate law, or Newton's law, depending on the range of the particle Reynolds number. In the present investigation the Reynolds number range for the glass beads was such that the intermediate law applied. For nonspherical polyethylene particles Pettyjohn and Christiansen's sphericity method was employed (*10*). Sphericity ϕ is defined as A_s/A_{ns}, where A_s is the surface area of a sphere having the same volume as the particle, and A_{ns} is the surface area of the particle (nonspherical). Therefore the sphericity of a nonspherical particle is always less than unity (see Table 1).

The terminal velocities of the particles used in this investigation were also determined by actual experiments in a 0.75-in. glass tube. Air or water was passed through the tube containing a single particle until the particle was suspended. The experimental values obtained were then corrected to the values in a 4-in. glass column by means of Ladenburg's correction for wall effect (*5*). Ladenburg's correction is applicable as long as the value of particle diameter to pipe diameter ratio is less than 0.1 (*4*).

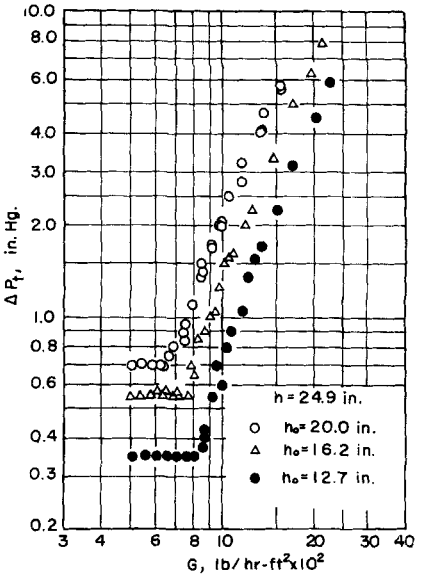

Fig. 6. Overall pressure drops across semifluidized beds (polyethylene sphere segments).

Table 3 lists all the terminal velocities of solid particles obtained by the three methods mentioned above.

It is seen that the calculated values are always lower than those obtained by extrapolation. The reasons for the discrepancy are discussed below. The assumption, that the voidage of the packed section is constant and is that of the least dense static bed ϵ_o, was probably true at low air velocities. The porosity of the packed section however tended to become slightly smaller than ϵ_o as the air velocity was increased. When all the solid particles were transported from the fluidized suspensions to the packed section, the height of the packed section was smaller than, instead of equal to, the initial static bed height, and the ratio h_{pa}/h_o would not reach unity. Consequently the values of terminal velocity obtained by the extrapolation of the curve to $h_{pa}/h_o = 1.0$ were obviously larger. Another

Table 5. Calculated and Observed Overall Pressure Drops

Particles	h, in.	h_o, in.	$D_p = 6/S_v$,* ft.	G, lb./hr.-sq. ft.	$\epsilon_{pa} = \epsilon_o$	ΔP_t, in. Hg: Equation (3)	Equation (2)	Observed	P_1, in. Hg	Air temp., °F.
80- to 100-mesh glass beads	24.7	17.3	0.000508	451.1	0.4386	9.89	21.6	23.2	55.0	70.7
Polyethylene sphere segments	24.9	20.0	0.00474	1,550.0	0.4893	3.18	6.30	5.5	34.3	68.0
Polyethylene cylinders	24.9	18.4	0.00935	1,483.5	0.4448	1.92	2.54	2.4	31.5	70.5

* D_p is defined elsewhere as the geometrical mean of particle diameter. In this case it is equal to $6/S_v$ as is defined in the Ergun equation.

Table 6. Ranges of Operating Conditions for Semifluidization Experiments

Particles	G, lb./hr.-sq. ft.	h, in.	h_o, in.	h_f, in.	h_{pa}, in.
80- to 100-mesh glass beads	10.9-551.5	24.7	17.3	17.3-36.5	0-13.4
Polyethylene sphere segments	497.5-2260.4	24.9	12.7-20.0	16.5-55.5	0-17.7
Polyethylene cylinders	658.7-2162.4	24.9	14.6-22.1	14.8-66.5	0-15.4

reason is that all materials had definite size distribution, even though very close size cut particles were used. The largest particles should have larger terminal velocity than the average ones; that is the maximum semifluidization velocity determined by the extrapolation method should be greater than that obtained for the completely uniform particles of average size. Since the average particle diameters were used in the calculation, the calculated values should be smaller than the extrapolated values which were evaluated when all the particles, including the largest ones, were transported from the fluidized section to the packed section. Furthermore, since the fluid along the center line of the column is moving faster than the fluid next to the walls, the particles near the walls may be falling downward while the particles in the center line of the column are already being held in suspension. This may be another argument for the extrapolated value to be larger than the calculated value. Table 3 also indicates that the calculated values are smaller than the observed values obtained from the actual suspension experiment. Needham and Hill (8, 9) investigated the velocity required to balance or suspend a particle situated in an upflowing fluid. Their results are of considerable interest since they shed some light on the mechanism of particle suspension in the fluidized systems. Their findings are that when both particle and pipe Reynolds numbers are in either the laminar or the turbulent flow, the ratio of the balancing velocity to the free fall terminal velocity approaches unity. On the other hand if one is in the laminar region while the other is in the turbulent region, the ratio departs considerably from unity.

For the present investigation both pipe and particle Reynolds numbers are listed in Table 4. The pipe Reynolds numbers were well in the turbulent region, while the single particle Reynolds numbers were in the intermediate region. Therefore the ratio of balancing velocity (G_t'') to terminal velocity (G_t) was larger than unity.

Pressure Drop Across Semifluidized Bed

The observed overall pressure drops across semifluidized beds are plotted against air rates in Figures 5 and 6. The constant pressure drop portions indicate that the packed sections have not yet formed.

Some difficulties were encountered in using Equation (3) to estimate the overall pressure drop in a semifluidized bed. The porosities in packed and fluidized sections cannot be measured directly. Although the porosity in the packed section can be assumed to be equal to that of the least dense static bed as in Equation (1), the Ergun equation, which is the basis of Equation (3), is known to be quite sensitive to the variation in bed voidage. A slight decrease in bed voidage due to the compression of the packed section will cause Equation (3) to deviate considerably.

The observed and calculated overall pressure drops for three particular readings are listed in Table 5 for comparison. Pressure drops in a fixed and fluidized bed were also measured in a separate experiment under the corresponding conditions, and Equation (2) was used to calculate ΔP_t. It is seen that either Equation (3) is not applicable to or the assumption that $\epsilon_{pa} = \epsilon_o$ is not valid for the solid-air systems in the present investigation.

Minimum Semifluidization Velocity

The minimum air velocity required for semifluidization depends on the fluid and particle characteristics, as well as the relative quantity of solid particles to the column size (h_o/h). The minimum semifluidization velocities for various particle beds and the h_o/h ratios can be obtained from Figures 5 and 6 at the points where the pressure drops begin to increase. If the ratio h_o/h is unity, the initial static bed height reaches the top sieve plate, and the semifluidization begins at the moment the bed starts to fluidize. Therefore as the ratio h_o/h approaches unity, the minimum semifluidization velocity G_s approaches the velocity for the onset of fluidization G_{mf}. On the other hand when the ratio h_o/h approaches zero, the semifluidization cannot be attained until the fluid velocity reaches the terminal velocity of the particles. The ranges of operating conditions for semifluidization experiments are tabulated in Table 6.

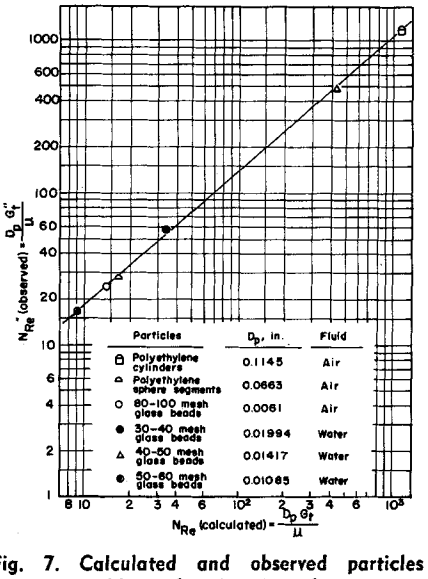

Fig. 7. Calculated and observed particles Reynolds numbers in 4-in. column.

Dimensionless Correlation for the Formation of Semifluidized Bed

Resorting to dimensional analysis and use of momentum and continuity equations for particulate fluidization, Fan and Wen derived the following expression (2):

$$F\left(\frac{h-h_o}{h-h_{pa}}, \frac{G-G_{mf}}{G_t-G_{mf}}\right) = 0 \quad (5)$$

The observed terminal velocities (or balancing velocities) G_t'' were always larger than the calculated values G_t as was previously mentioned. The experiments on terminal velocity studies with glass beads in water were also made. Figure 7 illustrates the linear relationship on log-log scale between N_{Re} and N_{Re}''. Thus balancing velocity may be evaluated from such a plot by calculating the terminal velocity with Stokes' law, or a modification of the law.

Figure 8 shows graphically the dimensionless relationship expressed by Equation (5) for all three kinds of particles used in the present investigation. A few of Fan and Wen's data (2) for glass bead-water systems are also presented after their calculated terminal velocities (G_t = 21,100 and 33,500 lb./hr.-sq.ft. for 50- to 60- and 40- to 45-mesh glass beads, respectively) were corrected to balancing velocities (G_t'' = 39,600 and 57,600 lb./hr.-sq.ft. for 50- to 60- and 40- to 45-mesh glass beads, respectively) by means of Figure 7.

The result shown in Figure 8 indicates that the relationships between the two factors $(h - h_o)/(h - h_{pa})$ and $(G - G_{mf})/(G_t'' - G_{mf})$ are nearly the same for any type of particle-fluid system, provided that the balancing velocity is used in the correlation.

CONCLUSIONS AND RECOMMENDATIONS

The results of the present investigation for solid-air systems were quite similar to those for solid-liquid systems which have been studied previously. The following conclusions may

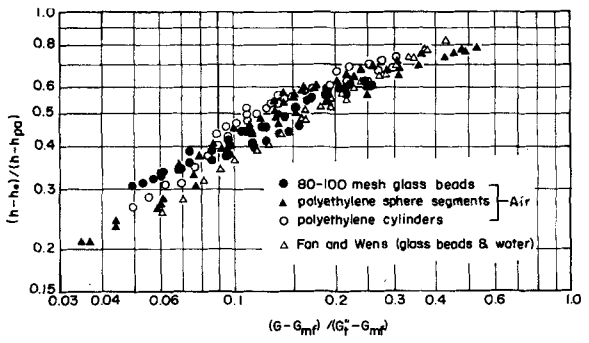

Fig. 8. Dimensionless correlation for semifluidized bed formation with balancing velocity.

be drawn based on the results of the present study:

1. The maximum height of a fully fluidized bed should be used in the correlation of semifluidization when the material balance equation $h_{pa} = (h_f - h)(1 - \epsilon_f)/(\epsilon_f - \epsilon_{pa})$ is used. It is valid for both solid-liquid and solid-gas systems provided one can make the assumption that the porosity of the packed section is constant and equal to the porosity of the least dense static bed. It is also applicable to any particle shape.

2. The usual assumption of identity between the velocity of fall of a particle in a fluid and the velocity required to balance a particle within the upflowing fluid is not valid. In the present investigation the balancing velocities were always larger than the calculated free fall terminal velocities. The latter are, again, always smaller than the terminal velocities determined by extrapolating the h_{pa}/h_o vs. G curve to $h_{pa}/h_o = 1.0$.

3. The overall pressure drop of a semifluidized bed can be found by summing up the pressure drop in the fluidized section and that in the packed section.

4. The minimum semifluidization velocity has a value somewhere between the onset velocity of fluidization and the maximum semifluidization velocity, depending on the value of the ratio h_o/h which has the limiting values of unity and zero. It can be obtained directly from a ΔP_t vs. G plot.

5. A unique dimensionless relationship exists between $(h - h_o)/(h - h_{pa})$ and $(G - G_{mf})/(G_t'' - G_{mf})$ for both liquid-solid and gas-solid systems of semifluidization. This arises from the fact that there is little interaction between the packed and fluidized sections.

Although some similar characteristics have been observed in the solid-gas and solid-liquid systems of semifluidization, the understanding of the solid-gas systems is still far from complete owing to the complexity of the aggregative bed pattern. Further investigation of the solid-gas systems is necessary before this similarity can be confirmed. The study should be extended to other types of gases and different solids with different particle sizes as well as mixed particle sizes.

NOTATION

A = cross-sectional area of empty column, L^2

D_p = particle diameter (geometrical mean), L

D_s = diameter of a sphere having the same volume as the particle, L

D_t = pipe diameter, L

F = function of

G = superficial mass velocity of fluid, $M\theta^{-1}L^{-2}$

G_{mf} = minimum fluidization velocity (onset velocity of fluidization), $M\theta^{-1}L^{-2}$, superficial

G_s = superficial minimum semifluidization velocity, $M\theta^{-1}L^{-2}$

G_t = superficial maximum semifluidization velocity, or calculated terminal velocity, $M\theta^{-1}L^{-2}$

G_t' = superficial maximum semifluidization velocity obtained by extrapolating h_{pa}/h_o vs. G curve to $h_{pa}/h_o = 1.0$, $M\theta^{-1}L^{-2}$

G_t'' = superficial terminal velocity obtained by fluidization experiment (corresponding to balancing velocity), $M\theta^{-1}L^{-2}$

g = gravitational constant, $L\theta^{-2}$

g_c = conversion factor, (lb. mass)(ft.)/(lb. force)(sec.)^2

h = overall height of semifluidized bed, L

h_f = height of fully fluidized bed, L

h_o = initial static bed height at the least dense condition, L.

h_{pa} = height of packed section in semifluidized bed, L

N_{Re} = calculated particle Reynolds number, D_pG_t/μ (dimensionless)

N''_{Re} = observed particle Reynolds number, D_pG_t''/μ (dimensionless)

P_1 = pressure at the bottom of the bed, FL^{-2}

ΔP = pressure drop across fully fluidized bed, FL^{-2}

ΔP_f = pressure drop across fluidized section in semifluidized bed, FL^{-2}

ΔP_{pa} = pressure drop across packed section in semifluidized bed, FL^{-2}

ΔP_t = overall pressure drop in semifluidized bed, FL^{-2}

$\left(\frac{\Delta P}{L}\right)_f$ = pressure gradient across fluidized bed, FL^{-3}

$\left(\frac{\Delta P}{L}\right)_{pa}$ = pressure gradient across packed bed, FL^{-3}

S_v = (surface area of particle)/(volume of particle), L^{-1}

u = superficial fluid velocity, $L\theta^{-1}$

u_t = terminal velocity of particle, $L\theta^{-1}$

W = total weight of particles in column, M

X = weight fraction of particles in packed section, dimensionless

Greek Letters

ϵ_f = porosity of fully fluidized bed, or porosity of fluidized section in semifluidized bed, dimensionless

ϵ_o = porosity of the least dense static bed under resting condition, dimensionless

ϵ_{pa} = porosity of packed section in semifluidized bed, dimensionless

μ = viscosity of fluid, $M\theta^{-1}L^{-1}$

ρ_f = density of fluid, ML^{-3}

ρ_s = density of solid particle, ML^{-3}

ϕ = sphericity of solid particle, dimensionless

LITERATURE CITED

1. Ergun, S., *Chem. Eng. Progr.*, **48**, 89 (1952).
2. Fan, L. T., and C. Y. Wen, *A.I.Ch.E. Journal*, **7**, 606-10 (1961).
3. Fan, L. T., Y. C. Yang, and C. Y. Wen, *ibid.*, **5**, 407 (1959).
4. Francis, A. W., *Physics*, **4**, 403 (1933).
5. Ladenburg, R., *Ann. Physik*, **23**, 447 (1907).
6. Leva, M., T. Shirai, and C. Y. Wen, *Genie Chim.*, **75**, No. 2, pp. 33-42 (1956).
7. Leva, M., "Fluidization," McGraw-Hill, New York (1959).
8. Needham, L. W., and N. W. Hill, *Fuel in Science and Practice*, **26**, 101 (1947).
9. Needham, L. W., and S. Lynch, *Trans. Inst. Chem. Engrs. (London)*, **23**, 93 (1945).
10. Pettyjohn, E. S., and E. B. Christiansen, *Chem. Eng. Progr.*, **44**, 157 (1948).

Manuscript received November 8, 1961; revision received October 30, 1962; paper accepted November 1, 1962. Paper presented at A.I.Ch.E. Baltimore meeting.